Materials Science and Engineering C 49 (2015) 541–548

Contents lists available at ScienceDirect

Materials Science and Engineering C

journal homepage: www.elsevier.com/locate/msec

Development and evaluation of elastomeric hollow fiber membranes as small diameter vascular graft substitutes

Ángel E. Mercado-Pagán [a], Yunqing Kang [a], Michael W. Findlay [b,c], Yunzhi Yang [a,d,*]

[a] Department of Orthopedic Surgery, Stanford University, Stanford, CA, USA
[b] Department of Plastic and Reconstructive Surgery, Stanford University, Stanford, CA, USA
[c] University of Melbourne Department of Surgery, Royal Melbourne Hospital, Parkville, VIC, Australia
[d] Department of Materials Science and Engineering, Stanford University, Stanford, CA, USA

ARTICLE INFO

Article history:
Received 8 August 2014
Received in revised form 10 December 2014
Accepted 14 January 2015
Available online 15 January 2015

Keywords:
Small diameter vascular grafts
Hollow fiber membranes
Phase inversion
Elastomers
Polyester urethanes

ABSTRACT

Engineering of small diameter (<6 mm) vascular grafts (SDVGs) for clinical use remains a significant challenge. Here, elastomeric polyester urethane (PEU)-based hollow fiber membranes (HFMs) are presented as an SDVG candidate to target the limitations of current technologies and improve tissue engineering designs. HFMs are fabricated by a simple phase inversion method. HFM dimensions are tailored through adjustments to fabrication parameters. The walls of HFMs are highly porous. The HFMs are very elastic, with moduli ranging from 1–4 MPa, strengths from 1–5 MPa, and max strains from 300–500%. Permeability of the HFMs varies from 0.5–3.5 × 10^{-6} cm/s, while burst pressure varies from 25 to 35 psi. The suture retention forces of HFMs are in the range of 0.8 to 1.2 N. These properties match those of blood vessels. A slow degradation profile is observed for all HFMs, with 71 to 78% of the original mass remaining after 8 weeks, providing a suitable profile for potential cellular incorporation and tissue replacement. Both human endothelial cells and human mesenchymal stem cells proliferate well in the presence of HFMs up to 7 days. These results demonstrate a promising customizable PEU HFMs for small diameter vascular repair and tissue engineering applications.

1. Introduction

While some degree of success has been attained with synthetic grafts with large diameters [1,2], a clinically-applicable small diameter vascular graft (SDVG), with diameters less than 6 mm, is still elusive [3]. Autologous grafts remain the gold standard for repair of small vessels, but their availability may be limited and their harvest increases patient morbidity [4]. Key characteristics of an ideal vessel substitute include mechanical compliance for the prevention of restenosis and hyperplasia, physical resilience for long-term patency, antithrombogenicity for clot inhibition, antifouling for protection of mechanical or chemical properties, and tailored degradation profiles to match gradual substitution with cellularized matrix [5,6].

Biologically-based materials, such as extracellular matrix (ECM) proteins, have been proposed and used for the design of vascular grafts. For example, both L'Heureux [7] and Dahl [8] developed tissue engineered blood vessels completely derived from ECM deposited by human smooth muscle cells. Clinical trials of this new construct by Lawson and Niklason recently led to its successful implementation in the repair of large kidney blood vessels in an adult patient [9]. However, the lengthy construction time of these grafts (around 10 weeks) significantly limits their clinical utility, particularly in the acute setting and there is still a paucity of data on the development of SDVGs with this technique.

Artificial SDVGs have been studied for more than two decades in an attempt to address the unmet clinical need for off-the-shelf small diameter vascular conduits. Several techniques have been applied in efforts to fabricate biocompatible SDVGs, such as electrospinning [10–12], phase inversion [13–22], molding [23–25], and combinations of methods [26–29], but no ideal technique exists to date. Polymers as a group offer significant versatility in vascular graft design due to their ease of customization and flexibility. Polylactic acid (PLA) [13], polycaprolactone (PCL) [14,15], poly(D,L-lactide-*co*-glycolide) (PLGA) [24], poly(glycerol sebacate) (PGS) [23,30], polyimides [17,18,20], polyurethanes [10,26,29], and other polymers [19,21] have been used successfully for the fabrication of candidate SDVGs. These SDVGs have also shown encouraging results. For example, Wen developed a phthalized chitosan tubular construct of less than 6 mm that showed good blood compatibility and reduced platelet adhesion [21]. More recently, Yadong Wang and coworkers developed a heparin-coated porous PGS vascular graft with an outer PCL shell [30]. Layering of PGS and PCL allowed for in vivo substitution with endothelial and smooth muscle cells, respectively, as the polymer matrix degraded.

Here, we present our methods and results for mechanical, degradation and cytotoxicity characterization of our biocompatible, biodegradable,

* Corresponding author at: Department of Orthopedic Surgery, Stanford University, 300 Pasteur Drive, Edwards R155, Stanford, CA 94305, USA.
E-mail address: ypyang@stanford.edu (Y. Yang).

http://dx.doi.org/10.1016/j.msec.2015.01.051
0928-4931/

elastomeric polyester urethane (PEU)-based hollow fiber membrane (HFM) as a potential SDVG. We use a simple, rapid phase inversion method to produce a continuous stream of elastic channeled HFM structures with properties suitable for vascular repair. By changing the fabrication parameters and the polyester content of the fibers by substitution with PLA, we can modify the properties of the HFMs. Phase inversion creates the permeable wall of the HFMs, which is useful for the diffusion of materials between the luminal and abluminal spaces. To manipulate the degradation profile and biocompatibility of the HFMs, we modified the PEU matrix with degradable polylactic acid. We sought to demonstrate that our rapid, customizable fabrication technique is capable of producing elastomer HFMs with comparable physical and chemical characteristics to native blood vessels so as to maximize the potential for their assimilation into new blood vessels following implantation and thus improve and enrich on current SDVG and tissue engineering platforms. Furthermore, we also conducted cytotoxicity studies with human endothelial cells and mesenchymal stem cells.

2. Materials and methods

2.1. Materials

A medical-grade PEU in pellet form (Estane® 5714F5, 90–200 kDa) was obtained from Lubrizol. D,L-Lactide was purchased from Ortec (Easley, SC). Erythritol (ET) was obtained from Alfa Aesar (Ward Hill, MA). Tin(II)-2-ethylhexanoate (TOC) was obtained from Santa Cruz Biotechnology (Santa Cruz, CA). 4′,6-Diamidino-2-phenylindole (DAPI) and dimethylsulfoxide (DMSO) were obtained from Fisher (Pittsburgh, PA). Rhodamine-phalloidin was obtained from Cytoskeleton (Denver, CO). 3-(4,5-Dimethylthiazol-2-yl)-2,5-diphenyltetrazolium bromide (MTT) was obtained from Sigma. An MSCGM™ BulletKit™, EBM™ (endothelial basal medium), and an EGM™ (endothelial growth media) SingleQuots™ Kit were purchased from Lonza. Dulbecco's Modified Eagle media (DMEM), fetal bovine serum (FBS), L-glutamine, antibiotic–antimycotic solution (penicillin–streptomycin–glutamine, PSG), phosphate buffer saline (PBS), and Hank's balanced salt solution (HBSS) were obtained from Invitrogen (Grand Island, NY).

2.2. Synthesis of 4-arm PLA

A branched PLA macromer was used to adjust the polyester content of the polymer stream while providing a networked matrix capable of reinforcing the mechanical properties of the resulting HFM. PLA was synthesized as described in our previous work [31]. For the synthesis of the PLA degradable copolymer, 30 g of D,L-lactide was added to a 500 mL flask and slowly melted under stirring. After melting, 1.22 g ET and 0.012 g TOC were added to the beaker. The reaction vessel was carefully heated to 100 °C under nitrogen atmosphere until all the ET dissolved. The temperature was then lowered and kept at 70 °C under nitrogen for 24 h. After the reaction was completed, the PLA-polyol product was precipitated in cold ethanol and dried under vacuum for 24 h. The theoretical calculated yield was 99.3%; the final yield for reactions was around 94.7%. ^{1}H NMR (300 MHz, $CDCl_3$, δ in ppm): 1.6 [d, 3H, CH_3], 5.2 [q, 1H, CH], 4.4 [t, 2H, CH_2]. Its calculated molecular weight was 3.65 kDa.

2.3. Hollow fiber membrane (HFM) fabrication

HFMs were fabricated by the phase inversion methods reported by Wen [32] with modification. For HFM production, a polyethylethylketone (PEEK) spinneret was constructed. The device and setup schematic are shown in Fig. 1A and B, respectively. The spinneret has two inner chambers separated by inserts. The inserts are fitted in the center by two steel cannulae which are lined concentrically along the bottom chamber and out a bottom exit. The ends of the cannulae are aligned so that both line up on the same horizontal plane. Water is pumped through the top chamber into the central cannula, while the polymer is pumped into the lower chamber, exiting between the cannulae. The HFM is collected in a water coagulant bath, where solvent exchange occurs for precipitation. Long, continuous HFMs can be fabricated until all the polymer solution is spent. After fabrication, the precipitated HFMs were kept overnight in a 25% glycerol in water to prevent flattening, and then dried for further use. For testing, 48 PLA/PEU HFMs were fabricated by varying polymer stream composition (30, 40, and 50%), PEU content in the polymer (100% and 90%), polymer stream temperature (70 and 130 °C), drop height (0 and 5 cm), and water bath temperature (20 and 35 °C). All HFMs were labeled with an "F" (for fiber) followed by five numbers representing the first digit of the variables mentioned above in order. For example, if a HFM was fabricated with a 30% polymer stream, containing 100% PEU and heated to 70 °C, a drop height of 5 cm, and a coagulant bath at 20 °C, the HFM was labeled "F-31752". From the pooled data, 5 different compositions, representative of the spectrum of variables used for this study, were picked for further testing as indicated in Table 1. Polymer solutions were prepared by dissolving the PLA and PEU in DMSO under heat and constant stirring.

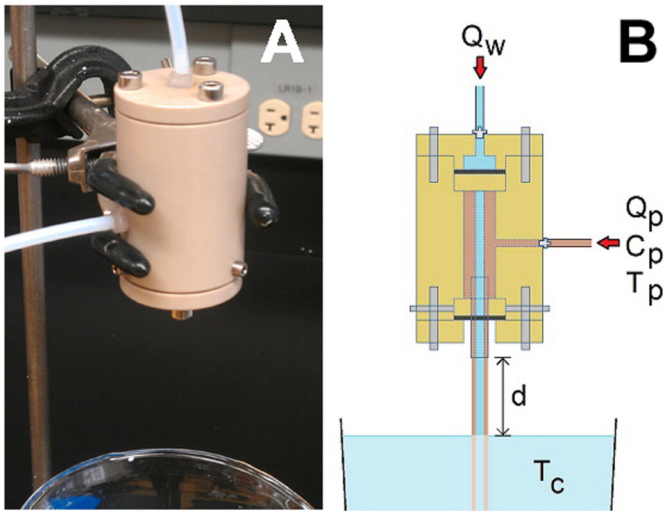

Fig. 1. Schematic for spinneret formation. (A) PEEK spinneret used for HFM fabrication. (B) Schematic for HFM fabrication, with relevant variables. Q_w: water flow, Q_p: polymer solution flow, C_p: polymer solution concentration, T_p: polymer solution temperature, T_d: coagulant bath temperature, d: drop height.

2.4. SEM imaging

Cross-sectional and longitudinal samples of HFMs were cut, fixed on aluminum pin mounts using carbon glue, and sputter-coated with gold for observation under SEM. The surface features of the composites were observed using a Hitachi S-3400 N VP SEM at an accelerating voltage of 15 keV. The chamber was kept in vacuum to avoid surface charging during the observation.

Table 1
Fabrication conditions for the HFMs[a].

HFM	C_p [vol.%]	C_u [vol.%]	T_p [°C]	d [cm]	T_c [°C]	Q_p [mL/min]	Q_w [mL/min]
F-31103	30	100	130	0	35	10	18
F-49703	40	90	70	0	35	12	19
F-41753	40	100	70	5	35	12	19
F-31752	30	100	70	5	20	10	18
F-59152	50	90	130	5	20	10	18

[a] Each of the five numbers of the HFM name correspond to the first digits of the values in the first five columns. C_p: solid concentration in the inlet polymer solution; C_u: PEU content within the total polymer content; T_p: polymer solution temperature; d: drop height; T_c: water bath temperature; Q_p: volumetric flow of polymer solution; Q_w: volumetric flow of water.

2.5. Tensile and suture retention testing

Mechanical testing for the HFMs was conducted using a Model 5944 test system equipped with a 100-N load cell (Instron Corporation, Norwood, MA). For testing, specimens were cut to a length of 10 cm. The samples were placed between two vertical clamps modified with 150 grit sandpaper (to prevent slippage) at a gage length of 5 cm. Samples were preloaded at 0.05 N before testing. The samples were then stretched at 10%/s until failure. Modulus, strength, and ultimate strain were recorded for all the samples. To test the suture retention strength, HFMs were cut to 40 mm-long samples. One end was fixed by the bottom stage clamp of the Instron tester, leaving a 20-mm gage length for testing, and the other end was connected to the movable top clamp by a 4–0 prolene suture (Ethicon, Inc.) inserted 5 mm from the sample end with a single loop. Samples were initially placed at a 0.1 N preload. All specimens were then pulled at a cross-head speed of 20 mm/min until failure. Maximum load was recorded.

2.6. Burst pressure

To test burst pressure, a syringe pump (New Era Pump Systems, Farmingdale, NY) with a 30-mL syringe was connected via Tygon® tubing to one end of the HFM, while the other end was connected to a pressure gauge (SSI Technologies, Janesville, WI). The pump was programmed to pump DI water at a rate of 1 mL/min until failure. The maximum pressure attained before failure was defined as the burst pressure.

2.7. Permeability study

Permeability measurements were carried out on the HFMs using a simplified version of a previously-reported method [33]. A chamber was constructed to allow countercurrent flow between the HFMs and the chamber interior. Flows were adjusted and monitored until conservation of flow rate was obtained in both inner and outer circuits. A 10 μg/mL fluorescent FITC-dextran solution was perfused through the inside of the HFMs at 0.1 mL/min, while clear water was perfused through the outside, on the space between the chamber and the HFMs. Outlet flows were collected. Exchange of the fluorescent marker was allowed to occur by diffusion through the HFM wall for 24 h. After reaching steady state, inlet and outlet concentrations were measured spectrophotometrically to determine the diffusive permeability of the HFMs according to the equation $P = J / (A \times \Delta C)$ [32], where P, J, A and ΔC are the diffusive permeability of the FITC-dextran (in cm/s), FITC-dextran mass flux from the chamber outlet (in mg/s), log mean membrane surface area of the HFM (in cm^2), and outlet concentration difference from the outlets (in mg/cm^3), respectively.

2.8. HFM degradation

To simulate the rate of degradation of HFMs in the body, HFM samples (2 cm in length) were carefully weighed and placed in 2 mL of HBSS (0.40 g/L KCl, 0.06 g/L KH_2PO_4, 8.00 g/L NaCl, 0.0477 g/L Na_2HPO_4, and 0.35 g/L $NaHCO_3$) at 37 °C for 8 weeks under sterile conditions, with time points every week, as performed in previous work [31]. HFM degradation was done in sealed containers to prevent both contamination and HBSS evaporation. Medical-grade polytetrafluoroethylene (PTFE, Zeus Inc., Orangeburg, SC) was used as a comparison to establish experimental continuity with our previously published hemocompatibility assays [34], which also used PTFE as a control. At each time point, the HFMs were collected and immediately weighed to record their wet weight, followed by 24-hours of vacuum drying to determine their dry weight. The degradation profile was then determined by dividing the remaining mass of polymer by the initial mass of the HFM segment. Sample HBSS supernatants were collected and filtered at 8 weeks for cell viability testing.

2.9. Cell culture

Human bone marrow-derived mesenchymal cells (hBMSCs) were purchased from Lonza Inc. (Allendale, NJ). Human umbilical vein endothelial cells (HUVECs) constitutively expressing green fluorescent protein (GFP) were generously donated by the late Dr. J. Folkman, Children's Hospital, Boston. hBMSCs were cultured in basal media, which consists of DMEM supplemented with 10% FBS, 200 mM L-glutamine, and 1% PSG. HUVECs were cultured in endothelial basal EBM-2 complemented with EGM-2 growth supplements as indicated by the manufacturer. Incubation of cells was done under standard conditions (5% CO_2, 95% humidity, and 37 °C). All cell experiments were carried out under sterile conditions.

2.10. Cell morphology on HFMs

HFMs were sterilized and conditioned by soaking in ethanol for 30 min, followed by PBS rinse for 30 min, and finally placing them in EBM-2 for 30 min. The HFMs were cut and flattened by pressing them between sterilized glass plates for 24 h. The flattened HFMs were affixed to the bottom of 24-well plates (BD Falcon) with sterilized silicon paste. hBMSCs and HUVECs were then seeded on top of the HFMs at 1×10^4 cells per well and allowed to grow for 48 h. In another experiment, an intact HFM was placed in a 3.5-cm dish (BD Falcon) and sealed on one end with silicon paste. Medium with a HUVEC concentration of 1×10^4 cells/mL was perfused through the other end, which was then immediately sealed with silicon paste. Afterwards, the HFM was covered with medium with a cell concentration of 1×10^4 cells/mL to observe cells seeding on the outside surface. The HFM was gently rotated manually every 20 min under sterile conditions for 8 h to allow homogeneous adhesion of cells.

For both experiments, HFMs were washed three times with PBS and cells were fixed with 4% paraformaldehyde in PBS at 37 °C for 20 min. After fixation, the paraformaldehyde solution was removed and cells were permeabilized using PBS containing 0.1% Triton X-100. HFMs were then rinsed with PBS and 200 μL of 100 nM rhodamine phalloidin solution (excitation and emission wavelength of 540 and 565 nm) was added for 30 min at ambient conditions to stain the actin filaments, followed by PBS washing. The cell nuclei were stained with 200 μL of DAPI solution (excitation and emission wavelength of 358 and 461 nm) for 30 s. The HFMs were washed twice with PBS. After this, the samples were placed inverted in a glass-bottom dish (In Vitro Scientific) for observation. An inverted fluorescent microscope (Zeiss Axioplan 2) with composite imaging functions was used to take images of the cultured cells.

2.11. Cell viability

HFM samples, each 1 cm in length, were placed in 48-well plates as described above. Next, HUVECs and hBMSCs were trypsinized and resuspended in their respective media at a concentration of 5×10^5 cells/mL. Then, 20 μL of cell suspension and 180 μL of media were directly added to each well to attain a final concentration of 1×10^4 cells per well. Cells were then allowed to grow for 7 days on the presence of HFMs, with time points at 1, 3, 5, and 7 days. Wells without HFMs and wells with 1-cm medical-grade PTFE tubing were used as controls. At each time point, cell proliferation was determined by using an MTT assay. A 5 mg/mL MTT stock solution in PBS was directly added to the media in the wells until diluted to a concentration of 0.5 mg/mL. The cells were then incubated for 3 h at 37 °C to allow reduction of MTT to purple formazan crystals. The media was then carefully removed, and crystals were dissolved in 200 μL DMSO for 30 min at 37 °C. Each well was thoroughly flushed to aid in formazan dissolution. Sample absorbance was then measured using an UV plate reader (BioTek) at 490 nm. All values were expressed as optical density, which indicates a measure of relative cell viability. To test the proliferation of the cells exposed to degradation products, cells at a concentration of 1×10^4

cells per well were cultured in suspensions consisting of 50% HBSS with degradation products of 8 weeks and 50% of EBM media for 3 days, with time points every 24 h. Cells cultured in 50% pure HBSS and 50% EBM were used as a control group. Viability of cells was then determined by the MTT assay described above.

2.12. Statistical analysis

All data is presented as average values ± standard deviation. Experiments were performed in triplicate ($n = 3$). Statistical difference was determined using one-way ANOVA analysis with Systat 12 (Systat Software Inc, Chicago, IL) followed by Tukey's post-hoc test ($\alpha = 0.05$).

3. Results

3.1. HFM fabrication and SEM observation

HFMs were successfully fabricated using a phase inversion method, as shown in Fig. 2. Fig. 2A shows their relatively small size after fabrication, with all HFMs being less than 1.5 mm in diameter. Fig. 2B shows a representative SEM image of an HFM cross-section. Higher magnification revealed a highly porous wall attained under precipitation (Fig. 2C), with pore sizes up to 75 μm. Fig. 2D1 to D5 shows the cross-sectional SEM images of the 5 selected HFMs, while Fig. 2E1 to E5 illustrates the inner surface of the HFMs. No obvious differences were observed in the texture and roughness of the HFMs.

3.2. Physical properties of HFM

HFM dimensions are shown in Table 2. In general terms, an increase in polymer concentration increased the diameter of the HFMs, with HFM ID increasing from 0.48 mm to 1.13 mm, OD increasing from 0.57 mm to 1.29 mm, and the thickness of the wall ranging from 0.09 to 0.16 μm. The results for physical properties of HFMs are shown in Fig. 3. Permeability of the wall varied from 3.4×10^{-7} to 3.1×10^{-6} cm/s and the burst pressure from 27.6 to 35.6 psi. The overall observed trend indicated a decrease in burst pressure with an increase in permeability (Fig. 3A). For example, permeability of the F-49703 HFM was lower than that of all the other HFMs, and its burst pressure was significantly higher to that of HFMs F-31103 and F-31752. Mechanical properties, in general, also increased with polymer concentration (Fig. 3B). Moduli ranged from 1.41 to 4.07 MPa, strength from 1.47 to 5.52 MPa, and max strains from 291 to 511%. The HFMs did not experience plastic deformation under stress and after failure. Suture retention testing showed that the HFMs could withstand loads from 0.8 to 1.2 N, with retention force increasing with HFM diameter (Fig. 3C).

Table 2
Dimensions of fabricated HFMs.[a]

HFM	ID [mm]	OD [mm]	Wall thickness [mm]
F-31103	0.48 ± 0.02	0.57 ± 0.01	0.09 ± 0.02
F-49703	0.77 ± 0.01	0.91 ± 0.01	0.13 ± 0.01
F-41753	0.89 ± 0.01	0.98 ± 0.02	0.09 ± 0.01
F-31752	0.97 ± 0.02	1.13 ± 0.01	0.16 ± 0.03
F-59152	1.13 ± 0.02	1.29 ± 0.01	0.16 ± 0.02

[a] ID: internal diameter; OD: outer diameter.

3.3. Degradation profiling

Degradation of the HFMs was conducted to determine stability of the material in vitro. For this, HFM segments were placed in HBSS to determine the amount of mass remaining after a period of 8 weeks, with time points every week. The results are shown in Fig. 4. The results showed a slow degradation profile for all HFM formulations, with 71 to 78% of the original mass remaining after 8 weeks. As expected, no significant change in mass was noted for the PTFE material at any time point and thus was not included in the degradation profiles. A slight decrease in pH was noticed at every time point for HFM formulations. Neither the degradation profiles nor the pH changes were considered statistically different at any time point for all groups. Swelling of HFMs did not increase more than 1% for all cases.

3.4. Cell morphology on HFMs

Both human umbilical vein endothelial cells (HUVECs) and human bone marrow stromal cells (hBMSCs) were stained for actin

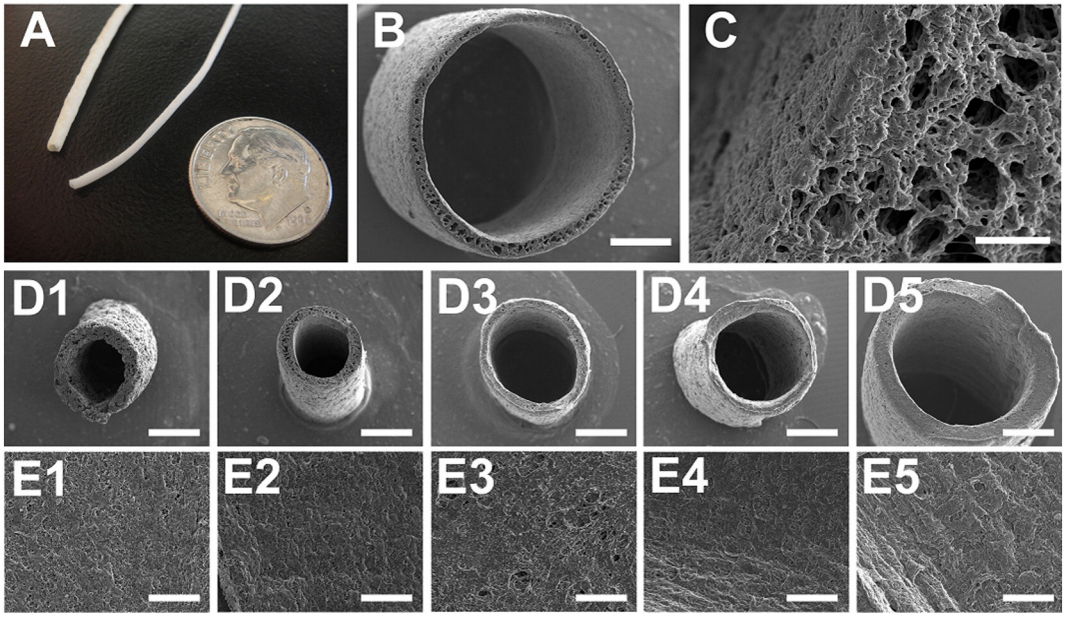

Fig. 2. HFM imaging. (A) Relative size of representative HFM. (B) Cross-sectional SEM image of representative HFM. Scale bar: 500 μm. (C) Magnification of HFM, showing porous wall. Scale bar: 25 μm. SEM images from (D1) to (D5) show cross-sections of evaluated SEM; (E1) to (E5) show SEM imaging of internal surfaces of HFM. For (D) and (E), 1: F-31103, 2: F-49703, 3: F-41753, 4: F-31752, and 5: F-59152. All HFMs were labeled with an "F" (for fiber) followed by five numbers representing the first digit of fabrication variables. The fabrication parameters and nomenclature of each HFM are listed in Table 1. Scale bar for cross-section: 500 μm; scale bar for inner surface: 250 μm.

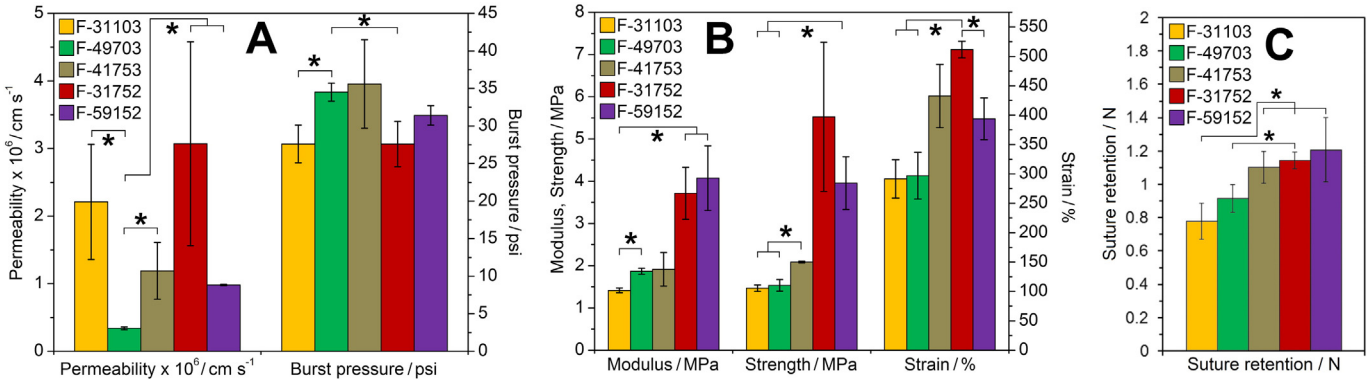

Fig. 3. Physical properties of HFMs. (A) Permeability and burst pressure of HFM. (B) Mechanical properties of HFM. (C) Suture retention force for HFMs. Samples were done in triplicate. One star indicates statistical difference between groups ($p < 0.05$).

(cytoskeleton) and DNA (nuclei) and imaged by fluorescent microscopy for visual inspection of cell morphology and attachment (Fig. 5). In Fig. 5A and B, the fluorescent images show spreading of HUVECs and hMSCs, respectively, along the surface of HFMs, demonstrating that cells could attach and proliferate well on the elastomer material. To test seeding of cells on the intact HFMs, HUVECs were also seeded on their inner and outer surfaces and observed by microscopy (Fig. 5C). The cells were then also stained and visualized under fluorescent microscopy. Imaging also confirmed that cells could also attach uniformly on intact HFMs, coating the inner and outer layers.

3.5. Cell viability

Viability and proliferation experiments were conducted to determine compatibility of the material on cells (Fig. 6). Results demonstrated that HUVECs proliferate on the surface of the material through 7 days, indicating non-toxicity of the material on endothelial cells (Fig. 6A). No significant differences were observed after 7 days when compared to medical-grade material or no-polymer (cell on well plates) groups. When cells were cultured with HFM degradation products of 8 weeks, all groups showed proliferation (Fig. 6B). After 5 days, HFM F-31752 showed a significant difference with the PTFE control group ($p = 0.005$), but returned again to comparable values at day 7. At day 7, only HFM F-59152 showed a significant difference with the PTFE group ($p = 0.007$), but in general all HFM groups had comparable values. For comparison purposes, the same experiment was conducted with hBMSCs, yielding similar proliferation patterns (Fig. 6C and D).

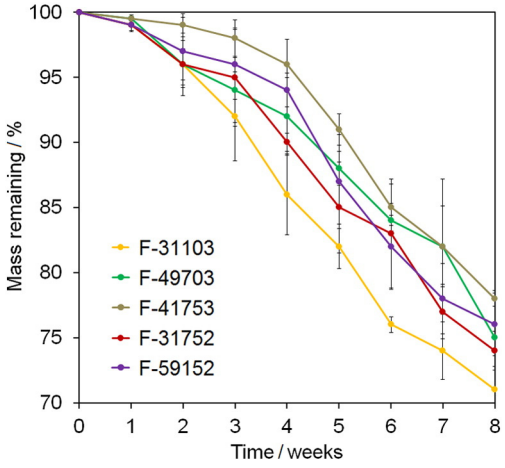

Fig. 4. Degradation patterns of the HFM polymers. Percentages are relative to the initial mass of the HFM. PTFE samples showed no degradation at any time point and thus were not included in the graph. Samples were done in triplicate.

4. Discussion

Two significant challenges in vascular tissue engineering are the production of small diameter neovessels and the vascularization of three-dimensional engineered constructs. In this work, we designed and produced a spectrum of mechanically-resilient HFMs as surrogate blood vessel grafts with tailored properties. Using a simple phase inversion method, we were able to produce a continuous HFM with superior tensile strength for good suture retention and to withstand both internal (blood pressure) and external (mechanical) pressures placed on vessel conduits when incorporated into the circulation and body. In vitro evaluation demonstrated the potential for HFMs to be biocompatible with endothelialized cells and tissues. Endothelialization of their lumen, combined with their suitable degradation profile should permit cell invasion in vivo and remodeling to produce a cellularized neovessel as the polymer matrix is substituted. Due to the inherent permeability of HFMs, they can also permit interluminal diffusion, thereby facilitating surrounding cell growth and neovascularization in support of potential 3D vascularized tissue engineering approaches.

Tensile and suture retention strength testing of the material was done to determine the mechanical resilience of the HFMs. The HFM showed sufficient elasticity to prevent permanent deformation and failure at low stresses. This characteristic permits HFMs to be sutured directly to blood vessels as interposition grafts. Our elastomeric HFMs matched or exceeded the mechanical properties of human blood vessels [35–37]. The results also showed that the permeability of the HFMs varied from 0.5–3.5 $\times 10^{-6}$ cm/s, well within the range of permeability of blood microvessels in the body (around 10^{-8} to 10^{-4} cm/s) [38]. HFM burst pressure varied from 25 to 35 psi, which is comparable to the expected burst pressure of saphenous veins, about 1600 mm Hg (31 psi) [39,40] and exceeding the properties of other proposed small vascular grafts, such as polyoctoate citrate grafts (1300 mm Hg) [40]. The size of the HFMs increased with polymer concentration, and expectedly, so did mechanical properties, such as tensile and suture retention strengths. The alignment and entanglement of these chains along the axis of force increase the ultimate strength of the HFMs [41]. Notably, permeability was the lowest in the groups with PLA addition. The formation of permeable walls in an HFM is a result of the exchange of organic solvent between the polymer and coagulant phases. It is possible then that the PLA, owing to the much lower molecular weight compared to the PEU, and thus lower hydrophobicity, decreases the entropy energy barrier for phase separation, leading to the formation of a denser, more stable layer [42]. The burst pressure seemed to correlate to the permeability of the sample (and thus, the void fraction) of the HFM wall. As the permeability decreased, the burst pressure seemed to increase, as in the example of HFM F-49703. It is possible that the void fraction reduced the ultimate amount of radial force that the walls can withstand before failure, which seems to correlate to the data. Suture retention force ranged from 0.8 to 1.2 N, which is sufficient for suturing

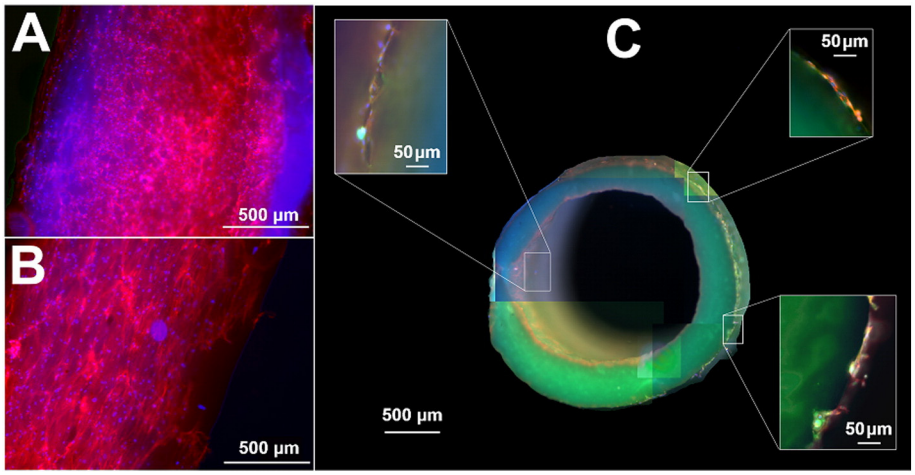

Fig. 5. Fluorescent imaging of cells attached to HFM films: (A) HUVECs and (B) hBMSCs. The image in (C) shows HUVEC attachment in the outer and inner surfaces of intact HFM. Red: rhodamine phalloidin, F-actin; blue: DAPI, nuclei. The green hue was due to the slight autofluorescence of polymer in the green channel. Scale bar for all images is 500 μm. (For interpretation of the references to color in this figure legend, the reader is referred to the web version of this article.)

small vessels and above the maximum retention force of similar grafts (0.5–0.7 N) [30,43].

For a graft to be successful, it has been postulated that it would have to be substituted eventually by endothelial and smooth muscle cells for complete restoration of functionality and patency of the blood vessel [30,44,45], although no definitive timeline has been defined. Some grafts might last a year or more after implantation [46], while there are grafts that have been completely substituted by cells in vivo [30] or in vitro [47] in as early as 3 months. Ideally, however, the rate of degradation of the engineered graft needs to meet the rate of ECM substitution to prevent premature failure as cells infiltrate the polymer matrix if it degrades too fast or inflammatory response if it degrades too slowly. In the case of the HFMs, phase inversion produces thin, permeable walls, which would facilitate bulk degradation of the polymer matrix concurrently with diffusion and cellular remodeling processes. PEUs, including Estane, have been shown to be susceptible to hydrolytic and enzymatic degradation in vitro [48,49]. Here, all polymer formulations degraded at a slow, quasi-linear rate, and increasing the polymer concentration slowed the degradation rate. This degradation behavior would be accelerated in the presence of the digestive enzymes of cells

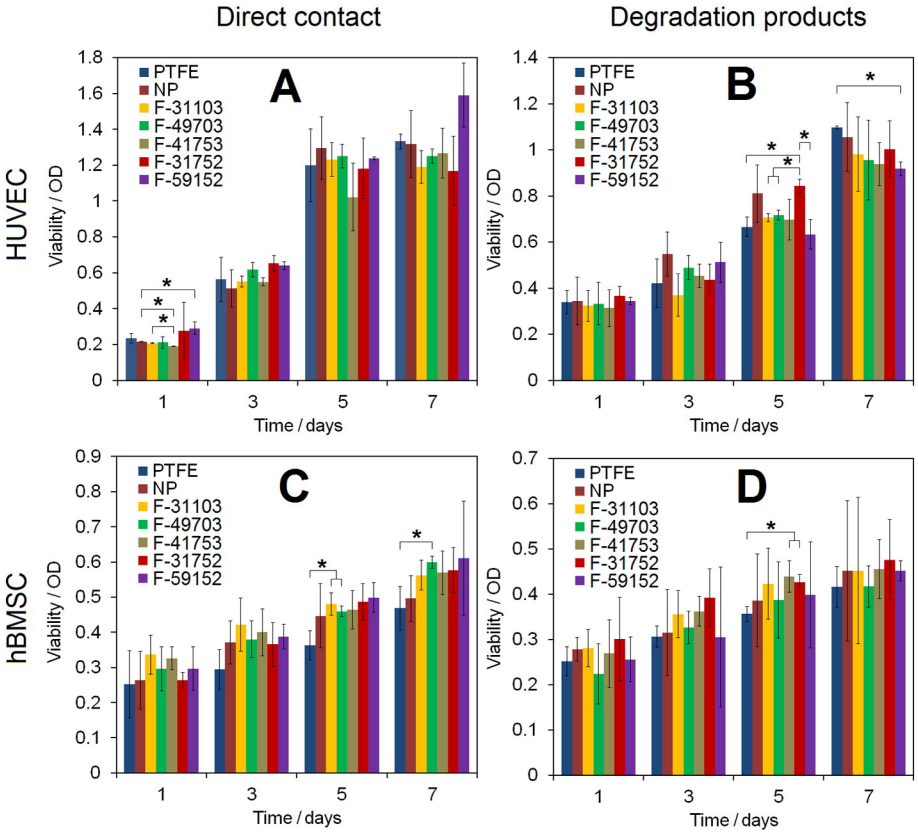

Fig. 6. Cell viability testing. The left column shows quantification of cell growth on HFM as determined by an MTT assay for (A) HUVECs and (C) hBMSCs. The right column shows proliferation of (B) HUVECs and (D) hBMSCs seeded with 50% EBM and 50% HBSS with degradation products at 8 weeks. PTFE refers to polytetrafluoroethylene samples; NP refers to group without polymer. Samples were done in triplicate. One star indicates statistical difference between groups ($p < 0.05$).

invading the matrix, so eventual endothelialization would assist in adjusting the degradation profiles to a desired rate. To support the growth of this endothelial layer after implantation, the vascular graft would have to have an associated permeability that would allow the exchange of wastes, oxygen, and nutrients through its wall. Our results showed that our HFM could potentially provide this exchange and sustain a viable endothelium.

Compatibility was tested by seeding HUVECs and hBMSCs on the HFMs and measuring their proliferation. These cells were also seeded in the presence of degradation products to determine their potential cytotoxicity. No significant toxic effects were noted in either experiment, and well-formed cell monolayers were formed on the surfaces of HFMs. Excellent cell compatibility is significant for two reasons. First, if the HFM graft were to be endothelialized in vitro for implantation in vivo as a self-remodeling graft, it would indeed be possible to allow a monolayer of endothelial cells to grow and consolidate around the inner or outer surfaces of the HFM. These cells would then remodel the degrading HFM into a cellularized neovessel. Second, if the HFM were to be used without pre-endothelialization, infiltrating cells from the body would still be able to reform the HFM into a patent vessel. Our compatibility results are also consistent with previous studies. For example, in one study, the effect of high-energy gamma irradiation on Estane–polydimethylsiloxane (PDMS) vascular grafts was evaluated. The procedure did not induce the release of cytotoxic products in cell culture media after 3 days. This was evidenced by a 3-(4,5-dimethylthiazol-2-yl)-2,5-diphenyltetrazolium bromide (MTT) viability assay using this media on L929 fibroblasts for 24 h [50]. Dabagh and coworkers did not observe fibroblast proliferation differences between Estane and PDMS-modified Estane surfaces after culture for 48 h [51]. Wagner [52,53] and Liska [54,55] developed degradable electrospun PEU vascular grafts comparable to commercially-available materials, showing good biocompatibility with cells in vitro and good mechanical properties, although complex PEU chemistry and fabrication were required to ensure this compatibility.

Although we have shown the potential of HFM to be used for vascular grafts, some limitations remain. The biocompatibility of the HFMs, for example, needs to be tested in vivo as well. Materials with slow degradation rates can become stiff from fibrous encapsulation, and inflammatory cells can induce neointimal hyperplasia [56], which has led to the development of techniques to minimize polyurethane inflammatory response [57]. However, Estane and PLA have been previously used with little to no adverse inflammatory responses. Earlier studies with Estane and polycaprolactone-polyurethane (PCLPU) porous meniscal replacements in a dog knee model showed tissue distributions similar to native collagenous tissue, with only a slight inflammatory response, encompassing macrophage and giant cell infiltration [58]. Alt and coworkers reported using stents with a low molecular weight PLA coating that released antithrombotic agents. The coated stents did not show increased inflammation when compared with uncoated stents in sheep and pig models [59]. We expect that tailored degradation profiles will yield substitution of the polymer with a cellularized matrix, reducing the impact of long-term body responses to the HFMs.

Estane has previously been used as a precursor material for engineered tissue substitutes due to its superior elastomer properties and compatibility [50,58,60,61]. However, its hard segment is based on methylene diphenyl isocyanate (MDI) monomers, which have been identified as precursors of 4,4′-methylenedianiline (MDA), a suspected carcinogen [62,63]. On the other hand, no significant adverse effects have been observed in a number of studies using this material. For example, histological examination of Estane–PDMS interpenetrated-network vascular grafts implanted in the carotid arteries of adult sheep showed only minor changes in organs, and no signs of systemic toxicity were observed after 6 and 24 months [61]. Nonetheless, in terms of clinical applicability, the risk needs to be eliminated by a longer-term study in large animals or selection of safer monomers for PEU synthesis. The extent and rate of cellular substitution of the HFM matrix need to be determined to optimize cellular remodeling. Moreover, the antithrombogenicity of the material needs to be measured and improved. For this, in vitro and in vivo testing of the material is essential; the properties of the HFMs in contact with blood will lead to optimization of the design to facilitate long-term viability after implantation. More experiments will be conducted to address these issues in future studies.

5. Conclusions

Elastomeric HFMs were successfully synthesized by a phase inversion method. The fabricated HFMs matched the physical and mechanical properties of native blood vessels or other artificial vascular grafts. An increase in polymer concentration increased mechanical properties, but slowed down the degradation rate. All HFM formulations showed a permeable wall, with burst pressure decreasing with an increase in permeability. A membrane wall that could allow material and cellular infiltration and assimilation, combined with a controlled degradation rate, would lead to HFM remodeling into an endothelialized neovessel after implantation. Biocompatibility exhibited in vitro also supports the feasibility of elastomeric HFMs as SDVG candidates. Future studies include development of novel elastomers for HFM synthesis and hemocompatibility evaluation of the elastomeric HFMs in vitro and in arterial interposition models. These encouraging initial results suggest that HFMs could be a powerful cost-effective future alternative for current SDVG technology and vascular tissue engineering applications.

Acknowledgments

We would like to acknowledge the financial support of the following agencies: NIH R01AR057837 (NIAMS), NIH R01DE021468 (NIDCR), and DOD W81XWH-10-1-0966 (PRORP). We would also like to thank Dr. Geoffrey C. Gurtner, from the Department of Plastic and Reconstructive Surgery at Stanford University, for his collaboration in this project. Finally, we are also grateful to Anthony Behn for his assistance in mechanical testing of samples, and Dr. Lydia-Marie Joubert from the Electron Microscopy Core at Stanford for use of, and assistance with, the Hitachi electron microscope.

References

[1] P. Klinkert, P. Post, P. Breslau, J. Van Bockel, Saphenous vein versus PTFE for above-knee femoropopliteal bypass. A review of the literature, Eur. J. Vasc. Endovasc. Surg. 27 (2004) 357–362.
[2] L.E. Niklason, R.S. Langer, Advances in tissue engineering of blood vessels and other tissues, Transpl. Immunol. 5 (1997) 303–306.
[3] Y. Song, J. Feijen, D. Grijpma, A. Poot, Tissue engineering of small-diameter vascular grafts: a literature review, Clin. Hemorheol. Microcirc. 49 (2011) 357–374.
[4] G.C. Lantz, S.F. Badylak, A.C. Coffey, L.A. Geddes, W.E. Blevins, Small intestinal submucosa as a small-diameter arterial graft in the dog, J. Invest. Surg. 3 (1990) 217–227.
[5] L.V. Thomas, V. Lekshmi, P.D. Nair, Tissue engineered vascular grafts — preclinical aspects, Int. J. Cardiol. 167 (2013) 1091–1100.
[6] S.E. Greenwald, C.L. Berry, Improving vascular grafts: the importance of mechanical and haemodynamic properties, J. Pathol. 190 (2000) 292–299.
[7] N. L'Heureux, S. Pâquet, R. Labbé, L. Germain, F.A. Auger, A completely biological tissue-engineered human blood vessel, FASEB J. 12 (1998) 47–56.
[8] S.L.M. Dahl, A.P. Kypson, J.H. Lawson, J.L. Blum, J.T. Strader, Y. Li, R.J. Manson, W.E. Tente, L. DiBernardo, M.T. Hensley, R. Carter, T.P. Williams, H.L. Prichard, M.S. Dey, K.G. Begelman, L.E. Niklason, Readily available tissue-engineered vascular grafts, Sci. Transl. Med. 3 (2011) 68ra69.
[9] ScienceDaily, 2013.
[10] H. Bergmeister, C. Grasl, I. Walter, R. Plasenzotti, M. Stoiber, C. Schreiber, U. Losert, G. Weigel, H. Schima, Electrospun small-diameter polyurethane vascular grafts: ingrowth and differentiation of vascular-specific host cells, Artif. Organs 36 (2011) 54–61.
[11] H. Inoguchi, I.K. Kwon, E. Inoue, K. Takamizawa, Y. Maehara, T. Matsuda, Mechanical responses of a compliant electrospun poly(L-lactide-co-ε-caprolactone) small-diameter vascular graft, Biomaterials 27 (2006) 1470–1478.
[12] K. Miyazu, D. Kawahara, H. Ohtake, G. Watanabe, T. Matsuda, Luminal surface design of electrospun small-diameter graft aiming at in situ capture of endothelial progenitor cell, J. Biomed. Mater. Res. B Appl. Biomater. 94B (2010) 53–63.

[13] N.M.S. Bettahalli, H. Steg, M. Wessling, D. Stamatialis, Development of poly(L-lactic acid) hollow fiber membranes for artificial vasculature in tissue engineering scaffolds, J. Membr. Sci. 371 (2011) 117–126.
[14] N. Diban, S. Haimi, L. Bolhuis-Versteeg, S. Teixeira, S. Miettinen, A. Poot, D. Grijpma, D. Stamatialis, Hollow fibers of poly(lactide-co-glycolide) and poly(ε-caprolactone) blends for vascular tissue engineering applications, Acta Biomater. 9 (2013) 6450–6458.
[15] N. Diban, S. Haimi, L. Bolhuis-Versteeg, S. Teixeira, S. Miettinen, A. Poot, D. Grijpma, D. Stamatialis, Development and characterization of poly(ε-caprolactone) hollow fiber membranes for vascular tissue engineering, J. Membr. Sci. 438 (2013) 29–37.
[16] X. Hu, H. Shen, F. Yang, J. Bei, S. Wang, Preparation and cell affinity of microtubular orientation-structured PLGA(70/30) blood vessel scaffold, Biomaterials 29 (2008) 3128–3136.
[17] H. Kawakami, T. Kanamori, S. Kubota, Development of a fluorinated polyimide hollow fiber for medical devices, J. Artif. Organs 6 (2003) 124–129.
[18] H. Kawakami, S. Nagaoka, S. Kubota, Gas transfer and in vitro and in vivo blood compatibility of a fluorinated polyimide membrane with an ultrathin skin layer, ASAIO J. 42 (1996) M871–M875.
[19] T.-Y. Liu, W.-C. Lin, L.-Y. Huang, S.-Y. Chen, M.-C. Yang, Surface characteristics and hemocompatibility of PAN/PVDF blend membranes, Polym. Adv. Technol. 16 (2005) 413–419.
[20] M. Niwa, H. Kawakami, M. Kanno, S. Nagaoka, T. Kanamori, T. Shinbo, S. Kubota, Gas transfer and blood compatibility of asymmetric polyimide hollow fiber, J. Biomater. Sci. Polym. Ed. 12 (2001) 533–542.
[21] Y. Qiu, N. Zhang, Q. Kang, Y. An, X. Wen, Fabrication of permeable tubular constructs from chemically modified chitosan with enhanced antithrombogenic property, J. Biomed. Mater. Res. B Appl. Biomater. 90B (2009) 668–678.
[22] M.-C. Yang, T.-Y. Liu, The permeation performance of polyacrylonitrile/polyvinylidine fluoride blend membranes, J. Membr. Sci. 226 (2003) 119–130.
[23] P.M. Crapo, Y. Wang, Physiologic compliance in engineered small-diameter arterial constructs based on an elastomeric substrate, Biomaterials 31 (2010) 1626–1635.
[24] K.R. King, C.C.J. Wang, M.R. Kaazempur-Mofrad, J.P. Vacanti, J.T. Borenstein, Biodegradable microfluidics, Adv. Mater. 16 (2004) 2007–2012.
[25] G. Vozzi, C. Flaim, A. Ahluwalia, S. Bhatia, Fabrication of PLGA scaffolds using soft lithography and microsyringe deposition, Biomaterials 24 (2003) 2533–2540.
[26] M. Ahmed, H. Ghanbari, B.G. Cousins, G. Hamilton, A.M. Seifalian, Small calibre polyhedral oligomeric silsesquioxane nanocomposite cardiovascular grafts: Influence of porosity on the structure, haemocompatibility and mechanical properties, Acta Biomater. 7 (2011) 3857–3867.
[27] M. Ahmed, G. Hamilton, A.M. Seifalian, Conf. Proc. IEEE Eng. Med. Biol. Soc. (2010) 251–254.
[28] A. de Mel, G. Punshon, B. Ramesh, S. Sarkar, A. Darbyshire, G. Hamilton, A.M. Seifalian, In situ endothelialisation potential of a biofunctionalised nanocomposite biomaterial-based small diameter bypass graft, Biomed. Mater. Eng. 19 (2009) 317–331.
[29] W. Xu, F. Zhou, C. Ouyang, W. Ye, M. Yao, B. Xu, Mechanical properties of small-diameter polyurethane vascular grafts reinforced by weft-knitted tubular fabric, J. Biomed. Mater. Res. A 92A (2009) 1–8.
[30] W. Wu, R.A. Allen, Y. Wang, Fast-degrading elastomer enables rapid remodeling of a cell-free synthetic graft into a neoartery, Nat. Med. 18 (2012) 1148–1153.
[31] Á.E. Mercado-Pagán, Y. Kang, D.F.E. Ker, S. Park, J. Yao, J. Bishop, Y.P. Yang, Synthesis and characterization of novel elastomeric poly (DL-lactide urethane) maleate composites for bone tissue engineering, Eur. Polym. J. 49 (2013) 3337–3349.
[32] X. Wen, P.A. Tresco, Fabrication and characterization of permeable degradable poly(DL-lactide-co-glycolide) (PLGA) hollow fiber phase inversion membranes for use as nerve tract guidance channels, Biomaterials 27 (2006) 3800–3809.
[33] M.J. Bridge, K.W. Broadhead, R.W. Hitchcock, K. Webb, P.A. Tresco, A simple instrument to characterize convective and diffusive transport of single hollow fibers of short length, J. Membr. Sci. 183 (2001) 223–233.
[34] Á.E. Mercado-Pagán, D.F.E. Ker, Y. Yang, Hemocompatibility evaluation of small elastomeric hollow fiber membranes as vascular substitutes, J. Biomater. Appl. 29 (2014) 557–565.
[35] A. Kurane, D.T. Simionescu, N.R. Vyavahare, In vivo cellular repopulation of tubular elastin scaffolds mediated by basic fibroblast growth factor, Biomaterials 28 (2007) 2830–2838.
[36] F. Pukacki, T. Jankowski, M. Gabriel, G. Oszkinis, Z. Krasinski, S. Zapalski, The mechanical properties of fresh and cryopreserved arterial homografts, Eur. J. Vasc. Endovasc. Surg. 20 (2000) 21–24.
[37] H. Yamada, F.G. Evans, Mechanical properties of circulatory organs and tissues, in: F.G. Evans (Ed.), Strength of Biological Materials, Williams & Wilkins, Baltimore, MD, 1970, pp. 114–130.
[38] C.C. Michel, F.E. Curry, Microvascular permeability, Physiol. Rev. 79 (1999) 703–761.
[39] G. Konig, T.N. McAllister, N. Dusserre, S.A. Garrido, C. Iyican, A. Marini, A. Fiorillo, H. Avila, W. Wystrychowski, K. Zagalski, M. Maruszewski, A.L. Jones, L. Cierpka, L.M. de la Fuente, N. L'Heureux, Mechanical properties of completely autologous human tissue engineered blood vessels compared to human saphenous vein and mammary artery, Biomaterials 30 (2009) 1542–1550.
[40] J. Yang, A.R. Webb, G.A. Ameer, Novel citric acid-based biodegradable elastomers for tissue engineering, Adv. Mater. 16 (2004) 511–516.
[41] J.J. Stankus, J. Guan, K. Fujimoto, W.R. Wagner, Microintegrating smooth muscle cells into a biodegradable, elastomeric fiber matrix, Biomaterials 27 (2006) 735–744.
[42] N. Zhang, Y. Huang, X. Wen, Formation of highly aligned grooves on inner surface of semipermeable hollow fiber membrane for directional axonal outgrowth, J. Manuf. Sci. Eng. 130 (2008) (021011-021011).
[43] S.P. Hoerstrup, G. Zünd, R. Sodian, A.M. Schnell, J. Grünenfelder, M.I. Turina, Tissue engineering of small caliber vascular grafts, Eur. J. Cardiothorac. Surg. 20 (2001) 164–169.
[44] K.L. Fujimoto, K. Tobita, W.D. Merryman, J. Guan, N. Momoi, D.B. Stolz, M.S. Sacks, B.B. Keller, W.R. Wagner, An elastic, biodegradable cardiac patch induces contractile smooth muscle and improves cardiac remodeling and function in subacute myocardial infarction, J. Am. Coll. Cardiol. 49 (2007) 2292–2300.
[45] A. Nieponice, L. Soletti, J. Guan, Y. Hong, B. Gharaibeh, T.M. Maul, J. Huard, W.R. Wagner, D.A. Vorp, In vivo assessment of a tissue-engineered vascular graft combining a biodegradable elastomeric scaffold and muscle-derived stem cells in a rat model, Tissue Eng. Part A 16 (2010) 1215–1223.
[46] E. Pektok, B. Nottelet, J.-C. Tille, R. Gurny, A. Kalangos, M. Moeller, B.H. Walpoth, Degradation and healing characteristics of small-diameter poly(ε-caprolactone) vascular grafts in the rat systemic arterial circulation, Circulation 118 (2008) 2563–2570.
[47] N. Bölgen, Y.Z. Menceloğlu, K. Acatay, İ. Vargel, E. Pişkin, In vitro and in vivo degradation of non-woven materials made of poly(ε-caprolactone) nanofibers prepared by electrospinning under different conditions, J. Biomater. Sci. Polym. Ed. 16 (2005) 1537–1555.
[48] B. Ratner, K. Gladhill, T. Horbett, Analysis of in vitro enzymatic and oxidative degradation of polyurethanes, J. Biomed. Mater. Res. 22 (1988) 509–527.
[49] W. Lemm, E.S. Bucherl, The degradation of some polyurethanes in vitro and in vivo, in: P. Ducheyne, G. van der Perre, A.E. Aubert (Eds.), Biomaterials and Biomechanics, Elsevier, Amsterdam, Netherlands, 1983, pp. 319–324.
[50] E. Briganti, T. Al Kayal, S. Kull, P. Losi, D. Spiller, S. Tonlorenzi, D. Berti, G. Soldani, The effect of gamma irradiation on physical–mechanical properties and cytotoxicity of polyurethane–polydimethylsiloxane microfibrillar vascular grafts, J. Mater. Sci. Mater. Med. 21 (2010) 1311–1319.
[51] M. Dabagh, M.J. Abdekhodaie, M.T. Khorasani, Effects of polydimethylsiloxane grafting on the calcification, physical properties, and biocompatibility of polyurethane in a heart valve, J. Appl. Polym. Sci. 98 (2005) 758–766.
[52] Y. Hong, S.-H. Ye, A. Nieponice, L. Soletti, D.A. Vorp, W.R. Wagner, A small diameter, fibrous vascular conduit generated from a poly(ester urethane)urea and phospholipid polymer blend, Biomaterials 30 (2009) 2457–2467.
[53] L. Soletti, A. Nieponice, Y. Hong, S.-H. Ye, J.J. Stankus, W.R. Wagner, D.A. Vorp, In vivo performance of a phospholipid-coated bioerodable elastomeric graft for small-diameter vascular applications, J. Biomed. Mater. Res. A 96A (2010) 436–448.
[54] S. Baudis, S.C. Ligon, K. Seidler, G. Weigel, C. Grasl, H. Bergmeister, H. Schima, R. Liska, Hard-block degradable thermoplastic urethane-elastomers for electrospun vascular prostheses, J. Polym. Sci. A Polym. Chem. 50 (2012) 1272–1280.
[55] S. Baudis, M. Schwarz, C. Grasl, H. Bergmeister, G. Weigel, H. Schima, R. Liska, (Bio) degradable urethane-elastomers for electrospun vascular grafts, Mater. Res. Soc. Symp. Proc. 1235 (2009) (1235-RR1203-1230).
[56] L. Li, C.M. Terry, Y.-T.E. Shiu, A.K. Cheung, Neointimal hyperplasia associated with synthetic hemodialysis grafts, Kidney Int. 74 (2008) 1247–1261.
[57] Z.-F. Lai, T. Imamura, N. Koike, Y. Kitamoto, Urokinase-immobilization suppresses inflammatory responses to polyurethane tubes implanted in rabbit muscles, J. Biomed. Mater. Res. A 76A (2006) 81–85.
[58] T.v. Tienen, R. Heijkants, J. De Groot, A. Schouten, A. Pennings, R. Veth, P. Buma, Meniscal replacement in dogs. Tissue regeneration in two different materials with similar properties, J. Biomed. Mater. Res. B Appl. Biomater. 76 (2006) 389–396.
[59] R. Herrmann, G. Schmidmaier, B. Markl, A. Resch, I. Hahnel, A. Stemberger, E. Alt, Antithrombogenic coating of stents using a biodegradable drug delivery technology, Thromb. Haemost. 82 (1999) 51–57.
[60] P.H. Robinson, B. Van Der Lei, H.J. Hoppen, J.W. Leenslag, A.J. Pennings, P. Nieuwenhuis, Nerve regeneration through a two-ply biodegradable nerve guide in the rat and the influence of ACTH4-9 nerve growth factor, Microsurgery 12 (1991) 412–419.
[61] G. Soldani, P. Losi, M. Bernabei, S. Burchielli, D. Chiappino, S. Kull, E. Briganti, D. Spiller, Long term performance of small-diameter vascular grafts made of a poly(ether) urethane–polydimethylsiloxane semi-interpenetrating polymeric network, Biomaterials 31 (2010) 2592–2605.
[62] P. Bruin, G. Veenstra, A. Nijenhuis, A. Pennings, Design and synthesis of biodegradable poly(ester-urethane) elastomer networks composed of non-toxic building blocks, Makromol. Chem. Rapid Commun. 9 (1988) 589–594.
[63] M. Szycher, V.L. Poirier, D.J. Dempsey, Development of an aliphatic biomedical-grade polyurethane elastomer, J. Elastomers Plast. 15 (1983) 81–95.